Gazi University Journal of Science
GU J Sci
25(2):519-532 (2012)

ORIGINAL ARTICLE

Dynamic Behaviors of a Two-Cylinder Four-Stroke Internal Combustion Engine

Halit KARABULUT[1,♠], Hakan ERSOY[2]

[1]*Gazi University, Technology Faculty, Department of Automotive Engineering 06500 Teknikokullar, Ankara*

[2]*Akdeniz University, Engineering Faculty, Department of Mechanical Engineering 07058 Kampus, Antalya*

Received: 07.12.2010 Revised: 08.09.2011 Accepted: 29.12.2011

ABSTRACT

In this study the vibrational aspects of a two-cylinder four-stroke internal combustion engine were studied. A dynamic model has been prepared with four degrees of freedom which are the translational vibrations of the engine block in vertical and horizontal directions, the rotational vibration of the engine block around the crankshaft center and the fluctuation of crankshaft angular speed. The model comprises forces and moments caused by inertial effects, hydrodynamic and dry frictions, startup moment, external load, gas pressures and mount forces. Vibrations of the engine block and fluctuation of crankshaft speed were optimized by using practical values. The inertia moment of the flywheel was found to be the dominant factor to minimize the angular speed fluctuation of the crankshaft. The gas force and the mass of the pistons were found to be the prevalent parameters contributing to the rotational and translational vibrations of the block respectively. It is observed that the vertical vibration of the block could be adequately minimized by means of exposing counterweights to the crankshaft, however, the counterweight induces a horizontal vibration while diminishing the vertical vibration. Therefore, in minimization of the translational vibrations of engine block, in addition to exposing counterweights, the piston mass should be very well minimized.

Key Words: Internal combustion engine, vibrations, crankshaft speed fluctuation

1. INTRODUCTION

From safety and comfort point of view, the most important problem of vehicles may be the vibration and noise. For the current time the noise generated by machines, including vehicles, is among the environmental concerns. In vehicles driven by piston engines, the principal source of vibration and noise is assumed to be the engine [1]. The impacts between parts of the piston-crank assembly are estimated as the main source of the engine noise [2]. Via inducing several physical effects such as material fatigues, impacts, frictions, heat generation, etc. the vibration causes failure of the systems taking part on the vehicle. Material fatigue is among the most important consequences of the vibration [3]. Vehicle vibration has also harmful effects on the human healthy. With respect to the frequency, amplitude and influencing period of the vibration, the human body experiences different degree of physiological and psychological discomforts such as weariness, back pain, distraction, annoyance, etc [4,5]. Vibrations have also the effect of increasing the dissipation of the mechanical energy, therefore, its minimization is an important part of the engine development researches.

The noise is generated by vibrations, however, the noise and vibration are different scopes of engineering studies. The vibrations generated by the engines have two principal causes, one is the inertia and unbalance of the rotating and translating components, the other is the working gas forces exerting on the piston [1,6-8].

♠Corresponding author, e-mail: halitk@gazi.edu.tr

Despite that the design of an engine without vibration is almost not possible; a dynamic simulation enables its minimization to a reasonable degree [9].

To suppress the unwanted vibrations of machines, principally three concepts have been devised which are vibration dampers, vibration isolators and vibration absorbers [10]. Dampers dissipate the energy of vibrating components via viscous shear. Isolators prevent the transmission of vibration from a machine component to the others. Vibration absorbers are devices generating inertia forces to push the main system from adverse direction.

In order to avoid the transmission of the engine vibrations to the chassis of the vehicles, vibration isolators are used [7,11]. In the literature of engine technology the vibration isolators are named as; engine mount, and most of them are made of rubber. A vehicle engine runs in a large enough speed range and generates vibration with different frequencies. An ideal vibration isolator is expected to isolate all of the vibrations. A rubber mount is able to isolate vibrations only in a limited frequency range[11]. Therefore, rubber mounts are designed to isolate the vibrations in a specified range of frequency. To obtain adequate performances in larger ranges of frequency, hydraulic mounts have been developed [12,13].

A dynamic model including all of the dynamic components of the engine and the chassis of the vehicle would enable a more reliable design tool for the engine mounts. However, since the development of such model would take too much time and require too much efforts, the engine and chassis are treated separately [14-16]. Even a dynamic model including the fundamental dynamic components of the engine beside the mounts is too complicated. Therefore, the engine mounts are designed via a simplified model named as rigid-body model [14-17]. In this model the engine is assumed to be a rigid mass having 6 degree of freedoms; three of them are translational displacements of the gravity center of the mass according to a (*x,y,z*) coordinate system, the others are rotations of the mass around the x, y and z axis. In rigid-body model the source of the vibration is predetermined harmonic excitation forces. The harmonic force is determined through a dynamic and thermodynamic analysis of an engine with a single piston and a stagnant block. The harmonic force can also be obtained through experiments.

Experimental investigations indicate that at minimum 10% of the engine power is wasted by inner frictions. Inner friction forces may be generated by viscosity of lubricants and the contact friction of metal surfaces[18-20]. The friction force induced by lubrication viscosity, named as hydrodynamic friction, is assumed to be linearly proportional to the velocity. The hydrodynamic friction is generated by the sliding motion of piston, and rolling motion of main journal and crank pin. The proportionality coefficient, named as viscous damping coefficient, was found to be not a simple constant, for both sliding and rolling motions. It is affected by speed and vibratory motion of sliding and rolling elements [21]. The contact friction generates a force similar to the dry friction. Its magnitude is related to the normal force exerting on the trust surfaces. The friction force generated by the piston ring is a dry friction and assumed to be non varying with piston speed [18]. The friction force appearing on the trust surface of the piston is assumed to be combination of hydrodynamic and dry friction forces.

The working gas pressure exerting on the piston may be calculated by means of a thermodynamic analysis or it may also be determined by experiments [9]. Especially the extremely large gas forces exerting on the piston at the beginning of expansion stroke about the upper dead center should be accurately predicted.

The theoretical prediction of specific properties of engine mounts is an important topic which is not treated in details. Karabulut et al. [22] devised a dynamic model enabling the prediction of the specific properties of mounts of a single-cylinder, four-stroke, internal combustion engine where the engine block was assumed to have two degrees of freedom as vertical motion and angular motion around the crankshaft center. In a second study Karabulut [23] has modified this dynamic model for a two-cylinder, four-stroke, in-line type engine, where the engine block has again two degrees of freedom as vertical motion and angular motion around the crankshaft center.

The present study is concerned with the dynamic modeling of a four-stroke, two-cylinder, in-line type diesel engine. In this study the motion of the engine block has three degrees of freedom as vertical motion, horizontal motion and angular motion around the crankshaft center. Together with the crankshaft speed fluctuation, the engine has four degrees of freedom. The dynamic model consists of the coupled equations of motion of pistons, piston connecting rods (conrod), crankshaft and cylinder block. As well as the common forces, the hydrodynamic damping forces exerting on pistons, main journals and crankpins were taken into account. Novelty of this study is the coupled treatment of the piston-crankshaft assembly and engine block. The model enables optimization of the mass of pistons and connecting rods, the minimization of the fluctuations of the crankshaft via assigning appropriate inertia moment for the flywheel, prediction of the frictional power and torque losses, optimization of counterweight masses, optimization of damping and spring constants of the mounts and predictions of the amplitudes of unavoidable engine block vibrations.

2. MATHEMATICAL MODEL

The coordinate systems used for the derivation of kinematic and dynamic relations are illustrated in Fig. 1, where *y*, y_c and Y indicate the vertical direction from up to down while *x*, x_c and χ are indicating the horizontal direction from right to left. The time (*t*) is the independent variable of the analysis. The crankshaft angle (θ), displacements of the crankshaft center (y_c)

and (x_c), and the angular displacement of the engine block around the crankshaft center (φ) are dependent variables of the analysis. Displacements of the piston-1 (x) and (y), displacements of the piston-2 (χ) and (Υ), and conrod angles (β) and (ϑ) are described by kinematic relations.

Displacements of the piston-1 and piston-2 (x), (y), (χ) and (Υ) are measured from the static position of the top dead centers. The angular displacement of the engine block (φ) is measured from the static position of the cylinder axis. The angular displacement of the crankshaft is measured from the vertical-upward direction that coincides with the cylinder axis. The static location of the crankshaft center is assumed to be the reference point of the translational displacements of the block (x_c) and (y_c).

The engine is assumed to be mounted on a rigid base via rubber mounts. The comparison of the static and any instantaneous positions of the piston-crankshaft assembly is shown in Fig. 1. Displacements of pistons-1 and piston-2 are

$$x = x_c + \left(R\cos\theta + \lambda\cos\beta\right)\sin\varphi \tag{1}$$

$$y = R + \lambda + y_c - \cos\varphi\left(R\cos\theta + \lambda\cos\beta\right), \tag{2}$$

$$\chi = x_c + \left[R\cos(\theta+\eta) + \lambda\cos\vartheta\right]\sin\varphi \tag{3}$$

$$\Upsilon = R + \lambda + y_c - \cos\varphi\left[R\cos\left(\theta+\eta\right) + \lambda\cos\vartheta\right] \tag{4}$$

Angles made by piston connecting rod with cylinder axis are

$$\beta = \arcsin\left(\frac{R}{\lambda}\sin\theta\right), \tag{5}$$

$$\vartheta = \arcsin\left[\frac{R}{\lambda}\sin\left(\theta+\eta\right)\right]. \tag{6}$$

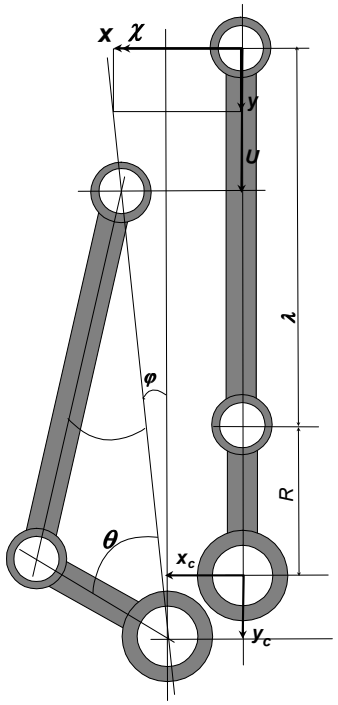

Fig. 1. Comparison of the static and an instantaneous position of the system

The position of any one of the pistons at any instant may be illustrated as shown in Fig. 2. The piston was assumed to be a lamped mass taking part at the center of piston pin. The stroke direction of pistons makes a φ angle with y axis. The forces exerting on piston-1 are the pressure force of working gas (F_W), pressure force of the crankcase (F_{CH}), dry friction force between the cylinder wall and side surface of piston-1 (F_u), the side force exerted by the cylinder wall (F_s), the force applied by conrod (F_L), the hydrodynamic force caused by damping effect of the lubricant ($F_{\mu 1}$) and

the force induced by crankpin friction (F_Ψ). The

$$m_p\ddot{x} = C_P\left[\dot{x}-\dot{x}_c-\left(R\cos\theta+\lambda\cos\beta\right)\cos\varphi\dot{\varphi}\right] + F_s\cos\varphi - F_L\sin\left(\beta-\varphi\right) - \left(F_W-F_{CH}-F_u\right)\sin\varphi + F_\Psi\cos(\beta-\varphi) \tag{7}$$

$$m_p\ddot{y} = -C_P\left[\dot{y}-\dot{y}_c-\left(R\cos\theta+\lambda\cos\beta\right)\sin\varphi\dot{\varphi}\right] + F_s\sin\varphi + \left(F_W-F_{CH}-F_u\right)\cos\varphi - F_L\cos\left(\beta-\varphi\right) - F_\Psi\sin(\beta-\varphi) \tag{8}$$

Using the same order that used for piston-1 above, the forces exerting on piston-2 may be written as: F_G , F_{CH} , F_r , F_δ , F_M , $F_{\mu 2}$ and F_Γ . The equations of motion of the piston-2 are

$$m_p\ddot{\chi} = C_p\left[\ \dot{\chi}-\dot{x}_c - \left(R\cos(\theta+\eta)+\lambda\cos\vartheta\right)\cos\varphi\,\dot{\varphi}\ \right] + F_\delta\cos\varphi - F_M\sin\left(\vartheta-\varphi\right) - \left(F_G-F_{CH}-F_r\right)\sin\varphi + F_\Gamma\cos(\vartheta-\varphi) \tag{9}$$

equations of motion of pistons-1 are

$$m_p\ddot{Y} = -C_P\left[\dot{Y}-\dot{y}_c-\left(R\cos(\theta+\eta)+\lambda\cos\vartheta\right)\sin\varphi\dot{\varphi}\right] + F_\delta\sin\varphi + \left(F_G-F_{CH}-F_r\right)\cos\varphi - F_M\cos\left(\vartheta-\varphi\right) - F_\Gamma\sin(\vartheta-\varphi) \tag{10}$$

From equation (7), the side force exerting on the piston-1 is chosen as,

$$F_s = \frac{F_L\sin\left(\beta-\varphi\right)}{\cos\varphi} + \left(F_W-F_{CH}-F_u\right)\frac{\sin\varphi}{\cos\varphi} - \frac{C_P}{\cos\varphi}\left(\dot{x}-\dot{x}_c-\left(R\cos\theta+\lambda\cos\beta\right)\cos\varphi\dot{\varphi}\right) + \frac{m_p}{\cos\varphi}\ddot{x} - \frac{F_\Psi\cos(\beta-\varphi)}{\cos\varphi} \tag{11}$$

From equation (8), the axial force appearing on the conrod of piston-1 is chosen as,

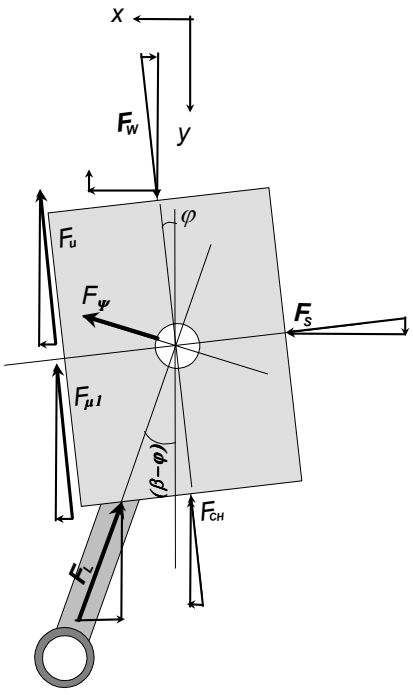

Fig. 2. An instantaneous position of the piston and forces exerting on it

$$F_L = -\frac{m_p}{\cos(\beta-\varphi)}\ddot{y} + (F_W - F_{CH} - F_u)\frac{\cos\varphi}{\cos(\beta-\varphi)} - \frac{C_P}{\cos(\beta-\varphi)}\left[\dot{y} - \dot{y}_c - (R\cos\theta + \lambda\cos\beta)\sin\varphi\,\dot{\varphi}\right] + F_S\frac{\sin\varphi}{\cos(\beta-\varphi)} - \frac{F_\Psi\sin(\beta-\varphi)}{\cos(\beta-\varphi)} \quad (12)$$

Similarly from equations (9) and (10) the side force and the conrod force exerting on piston-2 are chosen as,

$$F_\delta = \frac{F_M\sin(\vartheta-\varphi)}{\cos\varphi} + (F_G - F_{CH} - F_r)\times \frac{\sin\varphi}{\cos\varphi} - \frac{C_p}{\cos\varphi}\left[\dot{\chi} - \dot{x}_c - (R\cos(\theta+\eta) + \lambda\cos\vartheta)\cos\varphi\,\dot{\varphi}\right] + \frac{m_p}{\cos\varphi}\ddot{\chi} - \frac{F_\Gamma\cos(\vartheta-\varphi)}{\cos\varphi} \quad (13)$$

$$F_M = -\frac{m_p}{\cos(\vartheta-\varphi)}\ddot{\Upsilon} + (F_G - F_{CH} - F_r)\times \frac{\cos\varphi}{\cos(\vartheta-\varphi)} - \frac{C_P}{\cos(\vartheta-\varphi)}\left[\dot{\Upsilon} - \dot{y}_c - (R\cos(\theta+\eta) + \lambda\cos\vartheta)\sin\varphi\,\dot{\varphi}\right] + F_\delta\frac{\sin\varphi}{\cos(\vartheta-\varphi)} - \frac{F_\Gamma\sin(\vartheta-\varphi)}{\cos(\vartheta-\varphi)} \quad (14)$$

The dry friction forces exerting on the piston-1 and piston-2 may be described as [18],

$$F_u = \left[F_\infty + C_o|F_s|\right]\mathrm{sgn}(\dot{y}), \quad (15)$$

$$F_r = \left[F_\infty + C_o|F_\delta|\right]\mathrm{sgn}(\dot{\Upsilon}). \quad (16)$$

In equations (15) and (16), F_∞ is a constant friction force generated by piston rings.

The crank pin performs a rotational motion in the big-end bearing by means of rolling in it and induces a hydrodynamic moment. This moment is balanced by a reaction force applied by the gudgeon pin to the small-end bearing of the piston connecting rod. The reaction forces exerting on conrod-1 and conrod-2 may be described as,

$$F_\Psi = \frac{C_{km}}{\lambda}(\dot{\theta}+\dot{\beta}), \quad (17)$$

$$F_\Gamma = \frac{C_{km}}{\lambda}(\dot{\theta}+\dot{\vartheta}). \quad (18)$$

With respect to the crankshaft center, the reaction forces induce the moments:

$$M_{v1} = \frac{C_{km}}{\lambda}(\dot{\theta}+\dot{\beta})\left[R\cos\theta + \lambda\cos\beta\right] \quad (19)$$

$$M_{v2} = \frac{C_{km}}{\lambda}(\dot{\theta}+\dot{\vartheta})\times \left[R\cos(\theta+\eta) + \lambda\cos\vartheta\right] \quad (20)$$

where, the distance between the center of gudgeon pin and crankshaft is assumed to be the moment arm.

The big-end of the piston conrod performs a circular motion together with the crank pin while the other end is performing a translational motion with piston pin. The inertia force generated by the conrod in the direction of piston motion is accounted by means of increasing the piston mass as much as the half of the conrod mass. The other component of the conrod inertia force is approximately calculated via the equation of angular motion around the piston pin [1,9]. The equations of angular motion of piston conrods may be set as,

$$F_\beta = \frac{I_B}{\lambda}\ddot{\beta} \quad (21)$$

$$F_\vartheta = \frac{I_B}{\lambda}\ddot{\vartheta} \quad (22)$$

where, F_β and F_ϑ are tangential forces applied to the big-end of conrods by crank pins and reciprocal of F_β is illustrated in Fig. 3.

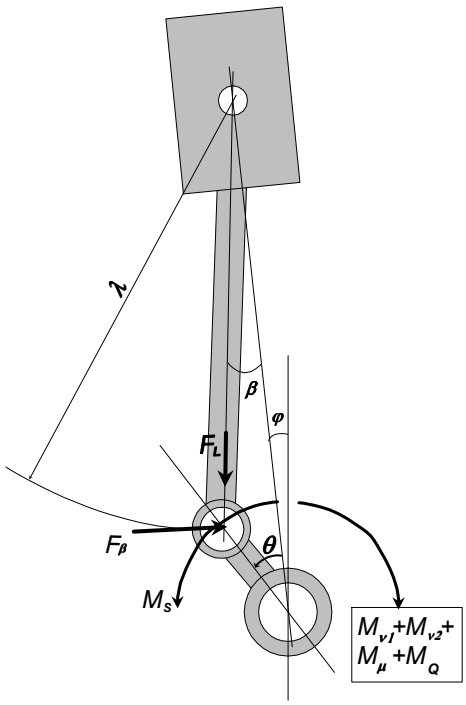

Fig. 3. Forces and moments contributing to the angular momentum of the crankshaft

The forces and moments contributing to the angular motion of the crankshaft are the piston conrod forces (F_L) and (F_M), tangential piston conrod forces (F_β) and (F_ϑ), moment of external load (M_Q), startup moment (M_S), moment of hydrodynamic friction appearing on the main journals (M_μ), moments of hydrodynamic frictions appearing on the crank pins (M_{v1}) and (M_{v2}). With regard to these contributions the equation of angular motion of the crankshaft may be written as,

$$\ddot{\theta} = -\ddot{\varphi} - \frac{R}{I_{CR}}\cos(\beta+\theta)F_\beta + \frac{RF_L}{I_{CR}}\cos\left[\frac{\pi}{2}-(\beta+\theta)\right] - \frac{RF_\vartheta}{I_{CR}}\cos(\vartheta+\theta+\eta) + \frac{RF_M}{I_{CR}}\cos\left[\frac{\pi}{2}-(\vartheta+\theta+\eta)\right] - \frac{1}{I_{CR}}\left(M_{v1}+M_{v2}+M_Q-M_S+M_\mu\right) \quad (23)$$

The forces and moments having contribution to the rotational vibration of the engine block are piston side forces (F_S), and (F_δ), hydrodynamic friction moments appearing in the main journals (M_μ), moments caused by the crank pin hydrodynamic frictions (M_{v1}) and (M_{v2}), startup moment (M_S), moment of torsional spring, and moment of torsional damper. The torsional spring and damper considered here are imaginer elements substituted for the engine mounts. The equation of angular motion of the block is,

$$\ddot{\varphi} = -\frac{C_C}{I_C}\dot{\varphi} - \frac{K_C}{I_C}\varphi - \frac{(R\cos\theta+\lambda\cos\beta)F_S}{I_C} - \frac{\left[R\cos(\theta+\eta)+\lambda\cos\vartheta\right]F_\delta}{I_C} + \frac{1}{I_C}\left(M_\mu+M_{v1}+M_{v2}-M_S\right) \quad (24)$$

Forces having influence on the translational vibration of the engine block are working gas pressure forces (F_W) and (F_G), crank case pressure (F_{CH}), the conrod forces (F_L) and (F_M), piston side forces (F_s) and (F_δ), piston dry friction forces (F_u) and (F_r), hydrodynamic friction forces appearing between pistons

and cylinders, the inertia forces generated by the counterweight masses taking part on the crankshaft, the damping and spring forces considered as the equivalent of mounts.

A conrod force (F_L) or (F_M) exerts on the crankpin and then divides into two components, one is tangential to the crank arm while the other is co-directional with crank arm. The force exerted to the engine block by the main journal is the combination of the tangential and co-directional components. That means, (F_L) and (F_M) are conducted to the engine block without any variation. Equations of the translational motion of the block in directions of x_c and y_c are

$$\ddot{x}_c = \frac{1}{m_e}\left[F_L \sin(\beta-\varphi) - F_{CH}\sin\varphi + F_W \sin\varphi - F_s\cos\varphi\right] + \frac{1}{m_e}\left[\ F_M \sin(\vartheta-\varphi) - F_{CH}\sin\varphi\right.$$
$$\left. + F_G \sin\varphi - F_\delta \cos\varphi\ \right] - \frac{C_p}{m_e}\left[\dot{\chi} - \dot{x}_c - \left(R\cos(\theta+\eta) + \lambda\cos\vartheta\right)\cos\varphi\,\dot{\varphi}\right] - \frac{C_P}{m_e}\left[\ \dot{x} - \dot{x}_c\right. \quad (25)$$
$$\left. - \left(R\cos\theta + \lambda\cos\beta\right)\cos\varphi\,\dot{\varphi}\ \right] - \frac{\sin\varphi}{m_e}\left(F_u + F_r\right) - \frac{K_x}{m_e}x_c - \frac{C_x}{m_e}\dot{x}_c + \frac{\omega^2}{m_e}\left[\ \sin\Omega\ m_u\ R_u + \right.$$
$$\left. \sin\Theta\ m_o\ R_o\ \right]$$

$$\ddot{y}_c = \frac{1}{m_e}\left[F_L\cos(\beta-\varphi) + F_{CH}\cos\varphi - F_W\cos\varphi - F_s\sin\varphi\right] + \frac{1}{m_e}\left[\ F_M\cos(\vartheta-\varphi) + F_{CH}\cos\varphi\right.$$
$$\left. - F_G\cos\varphi - F_\delta\sin\varphi\ \right] + \frac{C_P}{m_e}\left[\dot{Y} - \dot{y}_c - \left(R\cos(\theta+\eta) + \lambda\cos\vartheta\right)\sin\varphi\,\dot{\varphi}\right] + \frac{C_P}{m_e}\left[\ \dot{y} - \dot{y}_c - \right. \quad (26)$$
$$\left. \left(R\cos\theta + \lambda\cos\beta\right)\sin\varphi\,\dot{\varphi}\ \right] + \frac{\cos\varphi}{m_e}\left(F_u + F_r\right) - \frac{K_y}{m_e}y_c - \frac{C_y}{m_e}\dot{y}_c + \frac{\omega^2}{m_e}\left(\cos\Omega m_u R_u + \cos\Theta m_o R_o\right)$$

The mass of engine block (m_e) includes all of the masses except the piston masses. It is also eligible to use the total mass of the engine as m_e .

The variation of working gas pressure was experimentally obtained from a single cylinder, four stroke diesel engine [22,23]. To enable the use of data in computerization of the dynamic model, data were extrapolated with the Fourier series:

$$p(\theta) = \frac{A_0}{2} + \sum_{k=1}^{n}\left(A_k\cos k\theta + B_k\sin k\theta\right). \quad (27)$$

The values of A_k and B_k are tabulated in Table 1. Initial conditions to be used in numerical solution of the dynamic model are;

$\theta = 0$, $\dot{\theta} = 0$, (28 a,b)

$\varphi = 0$, $\dot{\varphi} = 0$, (29 a,b)

$x_c = 0$, $\dot{x}_c = 0$, (30 a,b)

$y_c = 0$, $\dot{y}_c = 0$. (31 a,b)

Table 1. Coefficients of Fourier expansion of working gas pressure[22,23]

k	0	1	2	3	4	5	6
A_k	1349.818	1030.205	801.032	657.438	564.255	434.054	339.754
B_k	–	193.499	203.204	166.924	165.394	176.483	143.554
k	7	8	9	10	11	12	13
A_k	271.190	217.846	161.010	127.082	93.664	74.861	50.122
B_k	127.997	114.023	102.304	85.144	73.474	63.190	54.484
k	14	15	16	17	18	19	20
A_k	39.469	25.794	20.503	11.320	8.553	3.135	2.598
B_k	44.804	38.206	32.473	27.892	24.056	20.131	17.283

3. INPUTS AND NUMERICAL SOLUTION

Inputs were determined with a comprehensive study including literature investigations, experimental operations and theoretical approximations. Before all, approximate dimensions of the engine components were determined and solid models of them were depicted. The mass and inertial mass moment of the dynamic components were then determined by means of a solid drawing software. The dry friction force (F_∞) is determined by a measurement and found to be consistent with ones given by Guzzomi et al., [18].

Dynamic dry friction coefficient of piston was taken from Ye et al., [24]. For Hydrodynamic friction, or hydrodynamic friction coefficient of the piston, Dawson et al. [25] suggested the Couette flow approximation. The hydrodynamic friction coefficient of the main bearings and big-end bearings of piston conrod were taken from Wang and Lim [21] and Durak et al., [26]. The predictions made for the same bearings via Couette flow is also found to be comparable with [21] and [26]. The crank angle between two pistons is assumed to be 2π rad, which enables repetition of the power strokes with equal crankshaft angles. The Inputs used in numerical applications are given in table 2.

Table 2. Specific values used in the analysis

Crank radius (m)	0.034
Conrod length (λ), (m)	0.118
Dynamic dry friction coefficient of piston (C_o)	0.05
Dry friction force generated by piston rings per piston $\left(F_\infty\right)$,(N)	55
Piston mass (kg)	0.7
Piston diameter (m)	0.086
Hydrodynamic friction constant of the piston (C_p), (Ns/m)	2.5
Counterweight mass per piston (kg)	0.7
Crank case pressure (p_{CH}), (bar)	101325
Mass inertia moment for articulation of Conrod around the gudgeon pin (I_B), ($\mathrm{m^2kg}$)	0.002
The sum of crankshaft and flywheel mass inertia moments (I_{CR}), ($\mathrm{m^2kg}$)	0.08
The total inertia moment of engine block for rotation around the crankshaft centre (I_C), ($\mathrm{m^2kg}$)	2.4
Hydrodynamics friction constant for the all of main journals and oil seals of the crankshaft, (Nms/rad)	0.01
The distance between Crankshaft counterweights mass center and crankshaft center (R_w, R_o), (m)	0.034
The total mass of engine block (m_e), (kg)	75
The mass of Piston plus the half of conrod mass, (kg)	0.7
Hydrodynamic friction constant for a big-end bearing (C_{km}), (Nms/rad)	0.0025
The angle between crank pins (η) (rad)	2π
Startup moment (M_S), (Nm)	50
Damping constant for torsional damper (C_C) (Nms/rad)	60
Stiffness of the torsional spring (K_C) (Nm/rad)	7000
Stiffness of the translational-vertical spring K_y (N/m)	500000
Stiffness of the translational-horizontal spring K_x (N/m)	500000
Damping constant for translational-horizontal damper (C_x), (Ns/m)	4000
Damping constant for translational-vertical damper (C_y), (Ns/m)	4000

Solution of dynamic model was obtained via an iterative prediction correction algorithm. By means of substituting the initial values, given by equations (28-31), into the kinematic relations (1-6); $x(0)$, $y(0)$, $\chi(0)$, $\Upsilon(0)$, $\beta(0)$ and $\vartheta(0)$ were calculated. Using derivatives of equations (1-6); $\dot{x}(0)$, $\dot{y}(0)$, $\dot{\chi}(0)$, $\dot{\Upsilon}(0)$, $\dot{\beta}(0)$, $\dot{\vartheta}(0)$ were calculated. Then,

using the second derivatives of equations (1-6), $\ddot{x}(0)$, $\ddot{y}(0)$, $\ddot{\chi}(0)$, $\ddot{\Gamma}(0)$, $\ddot{\beta}(0)$, $\ddot{\vartheta}(0)$, $\ddot{\mathrm{x}}(0)$, $\ddot{\mathrm{y}}(0)$, $\ddot{\chi}(0)$, $\ddot{\Gamma}(0)$, $\ddot{\beta}(0)$, $\ddot{\vartheta}(0)$ were approximately calculated. Using equations (11-22) approximate values of $F_s(0)$, $F_L(0)$, $F_\delta(0)$, $F_M(0)$, $F_u(0)$, $F_r(0)$, $F_\Psi(0)$, $F_\Gamma(0)$, $F_\beta(0)$, $F_\vartheta(0)$, $M_{v1}(0)$, and $M_{v2}(0)$ were calculated. Using derivatives of equations (11-22); $\dot{F}_s(0)$, $\dot{F}_L(0)$, $\dot{F}_\delta(0)$, $\dot{F}_M(0)$, $\dot{F}_u(0)$, $\dot{\mathrm{F}}_\mathrm{r}(0)$, $\dot{F}_\Psi(0)$, $\dot{F}_\Gamma(0)$, $\dot{F}_\beta(0)$, $\dot{F}_\vartheta(0)$, $\dot{M}_{v1}(0)$, and $\dot{M}_{v2}(0)$ were approximately calculated. Finally using equations (23-26) and their derivatives $\ddot{\theta}(0)$, $\ddot{\varphi}(0)$, $\ddot{x}_c$, $\ddot{y}_c(0)$, $\dddot{\theta}(0)$, $\dddot{\varphi}(0)$, $\dddot{\mathrm{x}}_\mathrm{c}(0)$, and $\dddot{y}_c(0)$ were approximately calculated. By means of reiterating the same numerical calculation made so far, for a number of times, rectification of the approximate results denoted above were performed. After this, by using equations:

$$\theta_1 = \theta_0 + \frac{\dot{\theta}_0}{1!}\Delta t + \frac{\ddot{\theta}_0}{2!}\Delta t^2 + \frac{\dddot{\theta}_0}{3!}\Delta t^3, \qquad (32)$$

$$\dot{\theta}_1 = \dot{\theta}_0 + \frac{\ddot{\theta}_0}{1!}\Delta t + \frac{\dddot{\theta}_0}{2!}\Delta t^2 \qquad (33)$$

θ_1 and $\dot{\theta}_1$ were predicted. In the same manner; φ_1, $\dot{\varphi}_1$, x_{c1}, $\dot{x}_{c1}$, y_{c1} and $\dot{\mathrm{y}}_{\mathrm{c1}}$ were predicted. The rest of the numerical procedure is repetition of the same operations. Magnitude of $\Delta\mathrm{t}$ may be determined by comparing results from the stability point of view. When a cubic Taylor expansion, such as equation (32), is used, a time step magnitude of $\Delta t = 1/5000$, found to be appropriate.

4. RESULTS AND DISCUSSION

Transient and steady behavior of the engine is illustrated in Fig. 4. The engine was initiated by means of rotating 1 radian via applying a 50 Nm startup moment. Up to that the crankshaft reaches to 314 rad/s mean speed, the engine was run without loading. After this, by applying an external load of 34.75 Nm, the mean speed of the crankshaft was stabilized at 314 rad/s or 3000 rpm. As seen from Fig. 4, during the unloaded transient running of the engine the mean speed displays a decelerating increase. Deceleration is caused by increasing friction losses with speed. At steady running conditions under 34.75 Nm external load, the crankshaft exhibits a 4% speed fluctuation corresponding to a 0.08 $\mathrm{m^2kg}$ combined inertia moment of crankshaft and flywheel. At lower values of steady mean speed, higher fluctuations were observed. To rather reduce the speed fluctuation of crankshaft, a massive increase in flywheel inertia moment was required. Piston masses was found to have too little influences on the speed fluctuation.

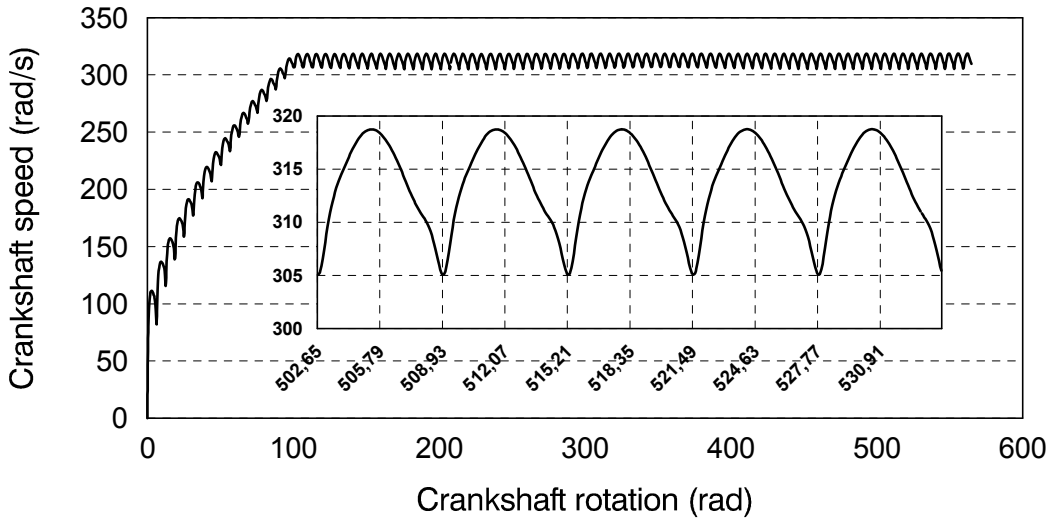

Fig. 4. Variation of the crankshaft speed

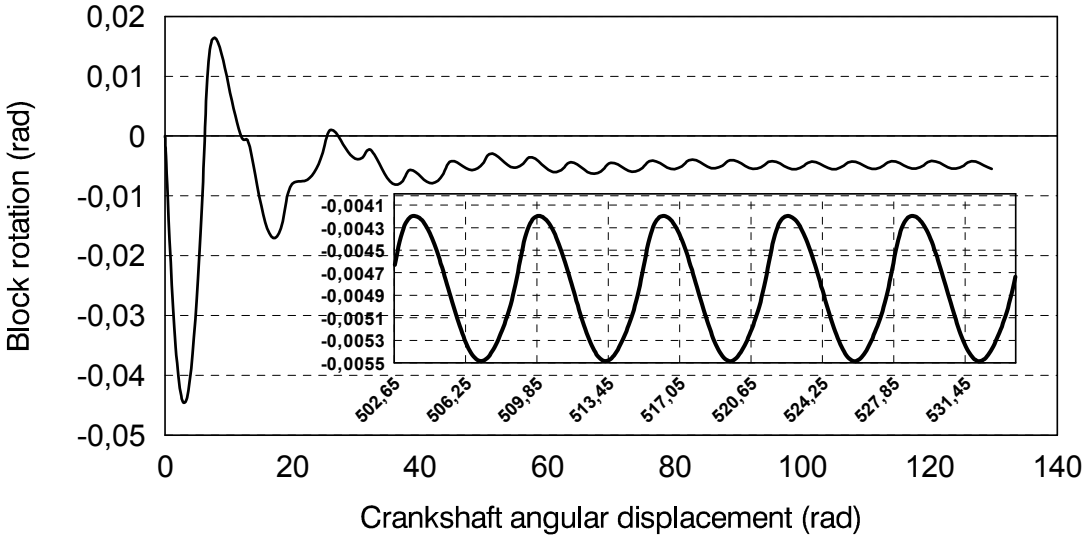

Fig. 5. Rotational vibration of the engine block

The rotational vibration of the engine block is illustrated in Fig. 5. The minimized rotational vibrations appearing at steady running conditions at 3000 rpm have an amplitude of 0.0013 radian. If the distance between crankshaft center and cylinder top is assumed to be 30 cm, there would be a 0.4 mm displacement at cylinder top. At initial oscillation however, its value is more than 15 mm. As seen from the magnified section in Fig. 5, the curve is smooth and there are no secondary vibrations. When running under an external load, the engine block slants backward. Fig. 5 indicates that, the location of the dynamic equilibrium is at about -0.005 radian backward to the static equilibrium point. This corresponds to a 1.5 mm displacement of the cylinder top. The principal cause of the rotational vibration of the engine block was found to be the working gas pressure. The influence of the piston mass was found to be insignificant. In this analysis the startup motor is assumed to be mounted on the engine block and it has a 18% effect of increasing the amplitude of initial oscillation.

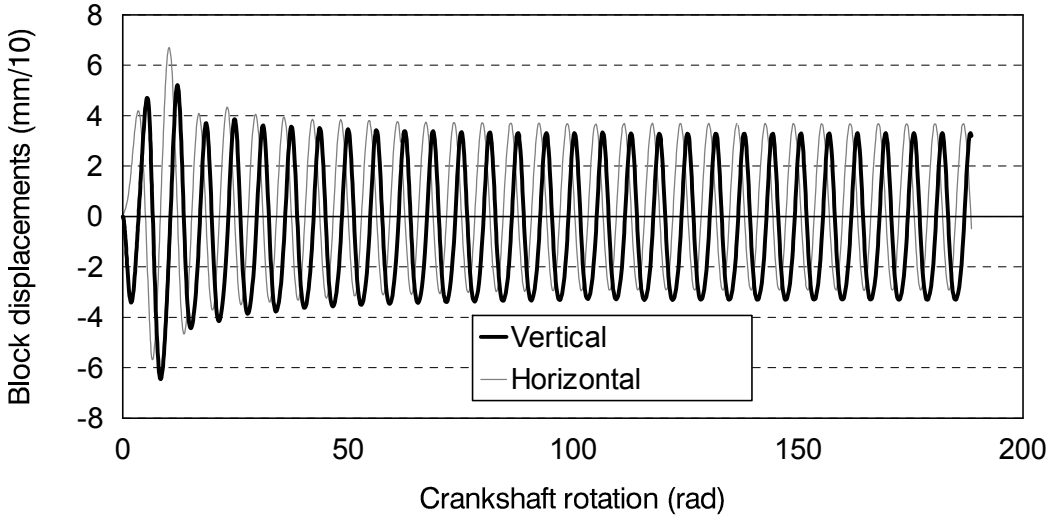

Fig. 6. The horizontal and vertical vibrations of the engine block

The horizontal and vertical vibrations of the engine block (crankshaft center) at transient and steady running conditions are illustrated in Fig. 6 for 75 kg block mass where the gray and dark lines indicate x_c and y_c respectively. The amplitude of largest oscillation appearing at startup period is about 1.2 mm. The transient oscillations of the engine block terminates after 5 revolutions. The amplitude of the minimized vertical and horizontal vibration at the steady running conditions are about 0.7 mm which are lowest possible values. The minimization is accomplished by means of exposing counterweights opposite to the crank pins on the crankshaft. Masses of counterweights exposed to crankshaft are equal to the half of piston mass, if their

distances from the crankshaft center are chosen equal to crank radius. When the masses of counterweights are rather increased, the amplitude of vertical vibration of engine block approaches to zero, however, the amplitude of horizontal vibrations tends to enlarge. It is seen that via imposing counterweight to the crankshaft, the translational vibration of the engine block can be minimized but not completely eliminated. To well reduce the vibration of an engine block in both directions, a very well minimization of the piston masses is inevitable. The relation,

$$m_p R = m_u R_u / 2 \tag{34}$$

enables prediction of the place of a counterweight approximately.

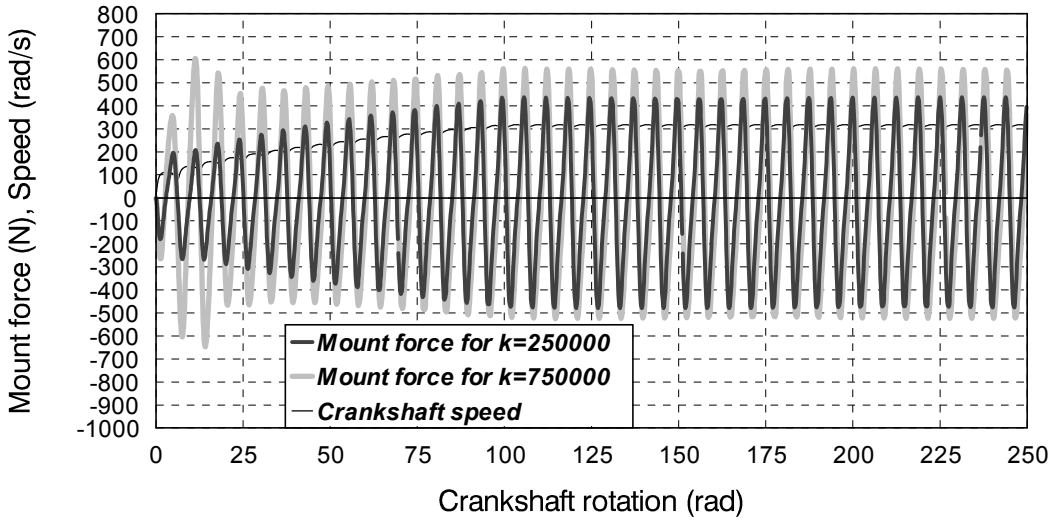

Fig. 7. Comparison of vertical mount forces obtained with two different stiffness

In Fig. 7, the vertical mount forces obtained for 250000 and 750000 N/m stiffness are compared. For 250000 N/m stiffness and 75 kg engine mass, the natural frequency of the block is estimated to be lower than 60 rad/s. On the other hand, the speed of the engine exceeds 100 rad/s within the first revolution of the crankshaft. Therefore, there occurs no periodic frequency coupling and the amplitude of mount force displays a smooth increase parallel to the crankshaft speed. For 750000 N/m stiffness however, the natural frequency of the block is not too low to avoid from coupling with operating frequency of the engine. Therefore, the mount force displays a jump at a speed of the crankshaft above 125 rad/s, where the amplitude of the force wave is about 1200 N as seen in Fig.7. When the damping constant of mount is increased, while the stiffness is the same, the jump of mount force is avoided. This indicates that, a mount may provide an adequate performance only, if there is an appropriate proportionality between its stiffness and damping constant.

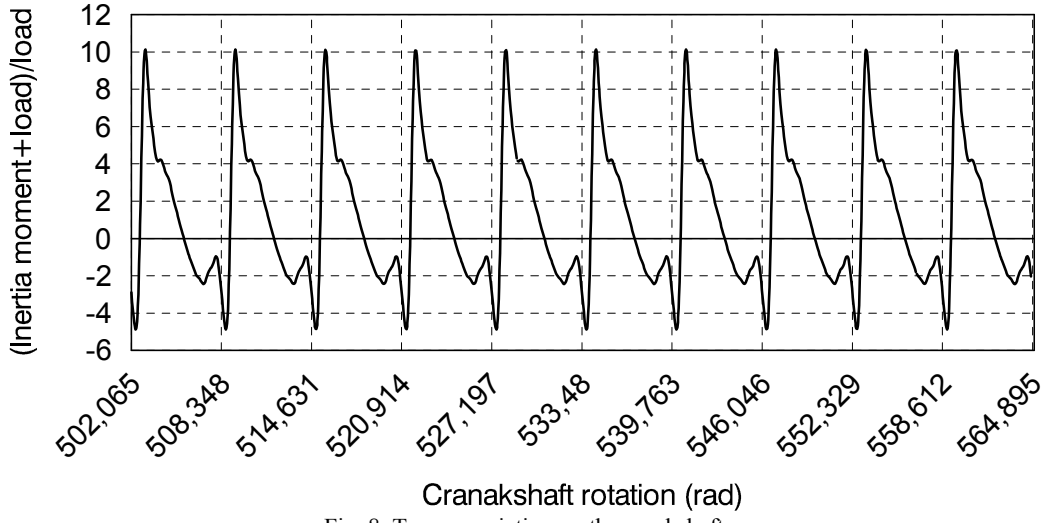

Fig. 8. Torque variation on the crankshaft

Fig. 8. illustrates the ratio of total moment to external load exerting on the crankshaft at steady operation of the engine. Total moment is the sum of inertia moment and external load which is 34.75 Nm. The highest value of the torque ratio appears within the startup process which is about 20. When the engine is reached to steady running speed and the external load is applied to the crankshaft, the torque ratio varies between -5 and 10. The magnitude of torque ratio is a clear indication of crankshaft failures appearing in diesel engines time to time.

5. CONCLUSION

A dynamic model was derived for a two cylinder four stroke engine and its dynamic behaviors were treated. The dominant factor causing rotational vibration of the engine block was found to be the side force which is a consequence of the gas force exerting on the piston. The translational vibrations in vertical direction were found to be generated mainly by piston masses. The vertical vibrations may be minimized by means of exposing counterweights to the crankshaft, however, its minimization is accomplished up to a certain degree since counterweights induce horizontal vibrations. Masses and places of the counterweights may be predicted by $m_p R = m_u R_u / 2$. A mount may provide an adequate performance only, if there is an appropriate proportionality between its stiffness and damping constant. The combined inertia moment of the flywheel and crankshaft was found to be the dominant factor to reduce crankshaft speed fluctuations. At dynamic conditions the place of the engine slightly differs from the static place. The inertia moment appearing on the crankshaft at transient and steady running of the engine is about 15 and 10 times the external load respectively. The rotational freedom of the block found to have a considerable effects on the crankshaft behavior.

6. REFERENCES

[1] Hofman D.M.W., Dowling D.R., "Modeling fully-coupled rigid engine dynamics and vibrations", ***1999 SAE Noise and Vibration Conference,*** Traverse City, Michigan, Proceedings, SAE Paper no. 1999-01-1749, 2:747-755, (1999).

[2] Cho S.H., Ahn S.T., Kim Y.H, "A simple model to estimate the impact force induced by piston flap", ***Journal of Sound and Vibration***, 255(2): 229-242, (2002).

[3] Chu C.C., "Multiaxial fatigue life prediction method in the ground vehicle industry", ***Int. J. Fatigue***, 19: 325-330, (1997).

[4] Paschold H.W., Sergeev A.V., "Whole-body vibration knowledge survey of U.S. occupational safety and health professionals", ***Journal of Safety Research***, 40: 171-176, (2009).

[5] Hostens I., Roman H., "Descriptive analysis of combined cabin vibrations and their effect on the human body", ***Journal of Sound and Vibration***, 266: 453-464, (2003).

[6] Boysal A., Rahneja H., "A torsional vibration analysis of a multi-body single cylinder internal combustion engine model", ***Applied Mathematical Modelling***, 21: 481-493, (1997).

[7] Yu Y., Naganathan N.G., Dukkipati R.V., "A literature review of automotive vehicle engine mounting systems", ***Mechanism and Machine Theory***, 36: 123-142, (2001).

[8] Wang R., "A study of vibration isolation of engine mount system", MsD Thesis, ***Concordia University***, The Department of Mechanical and Industrial Engineering, (2005).

[9] Hoffmann D.M.W., Dowling D.R., "Fully coupled rigid internal combustion engine dynamics and vibration, Part I: Model development", ***Journal of Engineering for Gas Turbines and Power***, 123: 677-684, (2001).

[10] Megahed S. M., Abd El-Razik A. K., "Vibration control of two degrees of freedom system using variable inertia vibration absorbers: Modeling and simulation", ***Journal of Sound and Vibration,*** 329: 4841-4865, (2010).

[11] FitzGerald D., "Focused engine isolation systems-the benefits", ***1997 SAE International Off-Highway And Powerplant Congress & Exposition,*** Milwaukee, Wisconsin, SAE paper no. 972777, 1-9, September (1997).

[12] Shangguan W.B., Lu Z-H., "Experimental study and simulation of a hydraulic engine mount with fully coupled fluid–structure interaction finite element analysis model", ***Computers and Structures***, 82:1751-1771, (2004).

[13] Wang L.R., Wang J.C., Hahiwara I., "An integrated characteristic simulation method, for hydraulic rubber mount of vehicle engine", ***Journal of Sound and Vibration***, 286: 673-696, (2005).

[14] Foumani M.S., Khajepour A., M. Durali, "Optimization of engine mount characteristics using experimental/numerical analysis", ***Journal of Vibration and Control***, 9: 1121-1139, (2003).

[15] Winton D.M., Dowling D.R., "Modal content of heavy-duty diesel engine block vibration", ***Society of Automotive Engineers,*** No: 971948, 621-630, (1997).

[16] Muller M., Siebler T.W., Gortner H., "Simulation of vibrating vehicle structures as part of the design process of engine mount systems and vibration absorbers", ***Society of Automotive Engineers,*** No: 952211, 1-11, (1995).

[17] Tao J.S., Liu G.R., Lam K.Y., "Design optimization of marine engine mount system", ***Journal of Sound and Vibration***, 235(3): 477-494, (2000).

[18] Guzzomi, A.L., Hesterman D.C., Stone B.J., "The effect of piston friction on engine block dynamics", ***Proceedings of the Institution of Mechanical Engineers Part K: Journal of Multi Body Dynamics***, 221: 277-289, (2007).

[19] Ciulli E., Rizzoni G., Dawson J., "Numerical and experimental study of friction on a single cylinder CFR engine", ***SAE International Congress and Exposition***, Michigan, 960357, 181-188, (1996).

[20] Livanos G.A., Kyrtatos N.P., "Friction model of a marine diesel engine piston assembly", ***Tribology***, 40: 1441-1453, (2007).

[21] Wang Y., Lim T.C., "Effects of viscous friction and non-friction damping mechanism in a reciprocating engine", ***Journal of Sound and Vibration***, 257(1): 177-188, (2002).

[22] Karabulut, H., Öztürk, E. and Çınar, C., ''Tek Silindirli dört zamanlı bir dizel motorunun dinamik modeli ve titreşimlerinin incelenmesi'', ***Gazi Üniversitesi Mühendislik-Mimarlık Fakültesi Dergisi, 26(1), 173-183, (2011)***

[23] Karabulut, H., Dynamic model of a two-cylinder four-stroke internal combustion engine and vibration treatment, ***International Journal of Engine Research***, doi: 10.1177/1468087412442618, 2012

[24] Ye Z., Zhang C., Wang Y., Cheng H.S., Tung S., Wang Q.J., He X., "An experimental investigation of piston skirt scuffing: a piston scuffing apparatus, experiments, and scuffing mechanism analyses", ***Wear***, 257: 8-31, (2004).

[25] Dowson D., Taylor C. M., Yang L., "Friction modeling for internal combustion engines", ***Tribology Series***, 31: 301-318, (1996).

[26] Durak E., Kurbanoğlu C., Bıyıkoğlu A., Kaleli H., "Measurement of friction force and effect of oil fortifier in engine journal bearings under dynamic loading conditions", ***Tribology International***, 36: 599-607, (2003).

NOMENCLATURE

A_k , B_k	Coefficients of Fourier expansion
C_C	Damping constant for the block torsional damper (Nms/rad)
C_o	Dry friction coefficient of piston surface
C_{km}	Hydrodynamic friction coefficient for big-end bearing (Nms/rad)
C_P	Hydrodynamic friction coefficient for piston (Ns/m)
C_x , C_y	Damping constant for the block translational damper (Ns/m)
F_{CH}	The pressure force exerting on the piston from back (N) (Fig. 2.)
F_L , F_M	Piston connecting rod axial forces (N) (Fig. 2.)
F_s , F_δ	Side forces exerting on pistons (N) (Fig. 2.)
F_u , F_r	Dynamic dry friction forces exerting on pistons (N) (Fig. 2.)
F_W , F_G	Working gas forces (N) (Fig. 2.)
F_Γ , F_Ψ	Side forces induced by crankpin hydrodynamic frictions (N) (Fig. 2.)
F_β , F_ϑ	Tangential forces exerting on big-ends (N), (Fig. 3.)
F_∞	Dry friction force generated by piston rings (N)
I_C	Inertia moment of the block with respect to crank center ($\mathrm{m^2kg}$)
I_{CR}	Combined inertia moment of the crankshaft and flywheel ($\mathrm{m^2kg}$)
K_C	Stiffness for imaginer torsional spring on the block (Nm/rad)
K_x , K_Y	Stiffness for imaginer translational spring on the block (N/m)
m_e	Total mass of the engine (kg)
m_p	Mass of the piston (kg)
m_u , m_o	Masses of the counterweights imposed to the crankshaft (kg)
M_Q	External load (Nm)
M_S	Start up moment (Nm)
M_μ	Total hydrodynamic friction moment for main journals (Nm)
$M_{\nu 1}$, $M_{\nu 2}$	Hydrodynamic friction moments generated by F_Ψ and F_Γ (Fig.2) (Nm)
p	Working gas pressure (Pa)

R	Crankshaft radius (m)
R_u , R_o	Distances between the crankshaft axis and counterweight (m)
x , y	Displacements of the piston-1 (m)
x_c , y_c	Displacements of the crankshaft center (m)
β , ϑ	Connecting rod angles with cylinder axis (rad)
φ	Angular displacement of engine block (rad)
θ	Crankshaft angle (Fig.1) (rad)
λ	Connecting rod lengths (m)
η	Phase angle between two pistons (rad)
Ω , Θ	Angles between the counterweights and y_c axis (rad)
Υ , χ	Displacements of the piston-2 (m)